Brucine Inhibits Proliferation of U87 Glioblastoma Cells by Targeting the G-quadruplexes in the c-Myb Promoter

Qiaochu Liu
The First Hospital of Jilin University
Di Huo
The First Affiliated Hospital of Harbin Medical University
Qunhui Wang
The First Hospital of Jilin University
Chuanqi Lv
The First Hospital of Jilin University
Ziqiang Liu
The First Hospital of Jilin University
Haijun Gao
The First Hospital of Jilin University
Yong Chen
The First Hospital of Jilin University
Gang Zhao (zhao_gangjlu@aliyun.com)
Department of Neurosurgery, The First Hospital of Jilin University, Changchun, China 2Clinical College, Jilin University, Changchun, China https://orcid.org/0000-0002-8416-9692

Research

Keywords: brucine, c-Myb, G-quadruplex, glioblastoma, U87

Posted Date: September 2nd, 2020

DOI: https://doi.org/10.21203/rs.3.rs-64115/v1

Version of Record: A version of this preprint was published at Journal of Cancer on January 1st, 2021.
See the published version at https://doi.org/10.7150/jca.53689.

Abstract

Background: The proto-oncogene c-Myb plays an important role in the proliferation of cells and its upregulation affects the development of glioblastomas. G-quadruplexes are secondary structures of DNA or RNA that usually form in the promoter region of oncogenes, including c-Myb, and regulate the expression of these genes. The traditional Chinese medicine brucine is a ligand of G-quadruplexes located in the promoter region of c-Myb. In this study, the U87 cell line was used both *in vitro* and *in vivo* to investigate the therapeutic effect and mechanism of action of brucine.

Methods: MTT assay and flow cytometry were used to determine the effect of brucine on the cell cycle, viability, and apoptosis of U87 cells. The effects of brucine on transcription and expression of c-Myb were determined through RT-PCR and western blotting. Dual-luciferase reporter assay and electrospray ionization-mass spectrometry were used to investigate whether brucine acts directly and binds G-quadruplexes in the promoter region of c-Myb, respectively.

Results: The results showed that brucine suppressed the growth of U87 cells *in vitro* by arresting the cell cycle and reducing the expression of c-Myb. Through the dual luciferase reporter assay, brucine was found to inhibit the expression of c-Myb by targeting the guanine-rich sequence that forms G-quadruplexes in the c-Myb promoter. Moreover, U87 tumors were suppressed by brucine in a tumor xenograft nude mice model.

Conclusion: The findings of the study indicate that brucine is a potentially effective medicine for treatment of glioblastomas.

Background

Although cerebral tumors account for only approximately 2% of all cancers, the morbidity and mortality contributed by these cancers are relatively high (1). Glioma is the most prevalent brain tumor and a major malignancy of the central nerve system in adults (2). Glioblastoma is one of the most deadly and aggressive types of gliomas with a World Health Organization grade of IV (3). Currently, tumor resection followed by radiotherapy and chemotherapy, typically temozolomide, is a common approach for managing patients with glioblastoma (4). However, reports have shown that the 2-year survival rate achieved by this therapeutic strategy is only 26.5%, with a median survival of 14.6 months (5). As it is one of the tumors most resistant to radiation and cytotoxic chemotherapy, patients with glioblastoma have a poor prognosis (6). Thus, effective targets and more practical treatments for glioblastoma are needed.

C-Myb is a proto-oncogene that encodes an important transcription factor relevant to the proliferation and differentiation of cells (7). This gene was first discovered as the mammalian cellular homolog of v-myb(8). Further studies have shown that this gene is highly expressed in many cancers, including colorectal tumors, T-cell leukemia, and most estrogen receptor-positive breast tumors(9). In addition, the amplification and upregulation of c-Myb have been observed in several glioblastoma cell lines(10). Genes activated downstream of c-Myb, such as Bcl-2, indicate that c-Myb function is associated with cellular survival(11). Furthermore, interactions between c-Myb and cyclin-D1 indicate that c-Myb is involved in the regulation of the cell cycle(12). Therefore, c-Myb may be a therapeutic target for glioblastomas.

Polynucleotide secondary structures, known as G-quadruplexes, are composed of several guanine tetrads that form layers through π-π stacking. G-quadruplexes can form rapidly under the appropriate physiological conditions and interact with specific proteins that have either a stabilizing or unfolding function(13). Many G-quadruplexes are located in guanine-rich RNA or DNA sequences, particularly in the promoter regions of oncogenes such as c-Myc(14). Approximately half of human genes have G-quadruplexes near their promoters(15). However, G-quadruplexes are not evenly distributed. In fact, G-quadruplexes are more prevalent in proto-oncogenes than in tumor suppressor genes(16). This interesting bias suggests that G-quadruplexes are important for regulating genetic expression, particularly that of proto-oncogenes. Studies of the function of G-quadruplexes in the metabolism of genetic information discovered in the past decade have shown the potential of G-quadruplexes to serve as regulators of genetic expression and therapeutic targets for specific cancers(17). For instance, c-Myb G-quadruplex structures negatively regulate the expression of the gene(18), suggesting that stabilization of these G-quadruplexes can lead to suppression of c-Myb transcription. Some small molecules that can interact with G-quadruplexes are expected to stabilize these DNA structures(19). According to a study by Huihui and colleagues, brucine may be a stabilizing ligand of G-quadruplexes in the promoter region of c-Myb(20). Therefore, the traditional Chinese medicine brucine may act as an effective suppressor of c-Myb by binding to the G-quadruplexes located in its promoter. In this study, we determined the anti-tumor effect and mechanism of action of brucine on a glioblastoma cell line.

Methods

Reagents and chemicals

Brucine was purchased from APExBIO (Boston, MA, USA). Antibodies were purchased from Abcam (Cambridge, UK). All other chemicals were purchased from MedChemExpress (Monmouth Junction, NJ, USA), unless indicated otherwise. The U87 human glioblastoma cell line was purchased from the American Type Culture Collection (Manassas, VA, USA).

Cell culture

Human U87 glioblastoma cells were cultured in Gibco Dulbecco's modified Eagle's medium (DMEM; Thermo Fisher Scientific, Waltham, MA, USA) supplemented with 10% fetal bovine serum and 100 U/mL of penicillin and streptomycin. Cells were maintained in a humidified incubator with 95% air atmosphere

and 5% CO_2 at a temperature of 37°C. Before the experiments, the cells were passaged for four generations.

MTT assay

U87 cells were harvested in the log phase and then adjusted to a density of 25,000 cells/mL. The cells were seeded into 96-well plates at 200 μL per well and incubated for 6 h. The medium of every three wells was replaced with 200 μL of DMEM containing 1, 0.5, 0.25, or 0 mM brucine. After 24-h incubation, 20 μL of MTT (5 mg/mL) was added to each well and the cells were incubated for an additional 4 h. After this, the supernatant was removed, 150 μL of dimethyl sulfoxide was added, and the 96-well plate was rocked on a shaker at an appropriate speed for 10 min. The optical density (15) of each well was measured at 492 nm using an enzyme-immunoassay instrument.

Flow cytometry assay

U87 cells were incubated with or without brucine (1, 0.5, 0.25, or 0 mM) for 24 h, harvested, and counted for use in subsequent assays. For the cell cycle assay, the cells were washed with cold (4°C) PBS and centrifuged at 1,000 rpm for 5 min. Then, 70% alcohol was added, and the cells were washed again with PBS and stained with propidium iodide (4) in the presence of 100 μL of RNase A for 30 min prior to analysis by flow cytometry. For the Annexin V/PI assay, the cells were washed with cold PBS. The supernatant was removed and then 1× binding buffer (100 μL) was added to each sample. After adding Annexin V (5 μL) and PI (5 μL), the volume of each sample was adjusted to 500 μL with 1× binding buffer. The cells were kept in the dark and analyzed through flow cytometry within 1 h.

Reverse transcription-polymerase chain reaction (RT-PCR)

U87 cells were incubated with or without brucine (1, 0.5, 0.25, or 0 mM) for 24 h. Total cellular RNA was extracted using TRIzol reagent according to the manufacture's protocol. After measuring the amount of total RNA with an enzyme-immunoassay instrument, RNase-free water was added to adjust the samples to the same density. Next, cDNA was acquired by reverse transcription using Superscript II Reverse Transcriptase according to the manufacturer's protocol. The SYBR Green method was used for performing RT-PCR on an iCycler (Bio-Rad, Hercules, CA, USA). cDNA (2 μL) from each sample was added as template to 18-μL reaction mixture containing 10 μL of Hieff qPCR SYBR Green Master Mix (YEASEN, Shanghai, China), 0.2 μM of each specific forward and reverse primer (Sangon Biotech, Shanghai, China), and 7.2 μL of RNase-free water. RT-PCR was performed according to the following protocol: 95°C for 5 min, 40 cycles of 95°C for 10 s, 60°C for 20 s, and 72°C for 20 s. At the end of the first round of RT-PCR, 80 cycles of 55°C + 0.5°C per cycle were used for melting curve analysis. GADPH was used as a control. The comparative CT method was used to determine relative expression levels.

Western blot assay

U87 cells were incubated with or without brucine (1, 0.5, 0.25, or 0 mM) for 24 h. The cells were harvested, washed with cold PBS, and homogenized on ice in RIPA lysis buffer with 1% 100× protease inhibitor cocktail. After centrifugation at 14,000 rpm for 15 min, the supernatants were collected, and protein levels were measured using the standard bicinchoninic acid assay. Thirty micrograms of protein from each sample were separated on a 10% sodium dodecyl sulfide-polyacrylamide gel and transferred to polyvinylidene fluoride membranes. The membranes were blocked with 5% fat-free milk containing Tris-buffered saline with Tween 20 for 2 h at 20°C. The membranes were separately incubated with primary antibodies against c-Myb, β-tubulin, BAX, cyclin-D1, caspase-9, and caspase-3 overnight at 4°C. After incubation, the membranes were washed with Tris-buffered saline with Tween 20 and incubated for 2 h at 20°C with anti-mice or anti-rabbit secondary antibodies according to the primary antibody. Finally, the protein bands were detected through Amersham electrochemiluminescence.

Dual luciferase reporter assay

Transfected cells were assessed using a Dual-Luciferase Reporter Assay System (Promega, Madison, WI, USA). The guanine-rich sequence, 5'-GGGCTGGGCTGGGCGGGG-3', located in the c-Myb promoter region was synthesized to replace the sequence from site KpnI to NheI of pGL3-basic (Promega)(20). Next, 293 cells were seeded in 12-well plates and co-transfected with 1.0 μg of moderated pGL3 or pGL3-basic and 0.2 μg of pRL-SV40 (Promega) according to the manufacture's protocol. After 48-h incubation following transfection, the cells were incubated with or without brucine (1, 0.5, 0.25, or 0 mM) for 24 h.

Electrospray ionization mass spectrometry (ESI-MS)

The sequence, 5'-GGGCTGGGCTGGGCGGGG-3', set as S1, and the complementary strand, set as S2, were synthesized (Sangon Biotech) with high-performance liquid chromatography. Annealing buffer was configured with Tris (10 mM), EDTA (1 mM), NaCl (50 mM), and pure water. DNA samples were divided into 4 groups: groups A and B with 0.1 mM S1 and groups C and D with 0.1 mM of both S1 and S2 in annealing buffer. Groups B and D were heated to 94°C, maintained for 2 min, and gradually cooled to room temperature. The four groups were separately divided into 4 subgroups with different concentrations of brucine (A1, B1, C1, and D1: 0 mM, A2, B2, C2, and D2: 5 mM, A3, B3, C3, and D3: 10 mM, and A4, B4, C4, and D4: 20 mM). Finally, the samples were detected with SYNAPT G2-Si (Waters, Milford, MA, USA).

Tumor xenograft model in nude mice

Female nude mice (25–30 g, 6 weeks old) were purchased from the Animal Center of Chinese Academy of Sciences (Shanghai, China). All mice were allowed free access to food and water under controlled conditions (12/12 h light/dark cycle with humidity of 60% ± 5% and temperature of 22 ± 3°C). All experimental protocols were approved by the Ethics Committee of the First Hospital of Jilin University and its institutional animal-care committee. Approximately 5×10^6 U87 cells were suspended in 200 μL ECM-gel (Sigma-Aldrich, St. Louis, MO, USA) with 50% 1× PBS and injected into the subcutaneous right forelimb axilla of 6-week-old female nude mice. After two weeks, mice with palpable tumors were

randomly placed into two groups for treatment with either brucine or an equivalent volume of normal saline (NS). Mice in the experimental group were intraperitoneally injected with brucine (10 mg/kg) every 24 h and for 10 days. During treatment, body weights of mice were monitored and tumor sizes were measured every two days. After treatment, all mice were sacrificed and their tumors were resected and stored at –80°C. All studies were performed under the China Association for the Accreditation of Laboratory Animal Care guidelines for humane treatment of animals and adhered to national and international standards.

Data analyses

Data analyses were conducted using GraphPad Prism 7 software (GraphPad, Inc., La Jolla, CA, USA). The results were presented as the mean ± standard deviation. Student's *t* test or one-way analysis of variance was used to compare two or more than two groups, respectively. $P < 0.05$ was considered as statistically significant.

Results

Brucine reduces U87 cell viability

The effect of brucine on U87 cell viability was assessed using MTT assay. As shown in Figure 1, brucine negatively affected the total survival of cells. Specifically, the quantity of living cells was reduced in a dose-dependent manner. Particularly, at a relatively high concentration (0.5 or 1.0 mM), U87 cells were significantly suppressed compared with those in the control (0 mM) group.

Brucine affects the U87 cell cycle and apoptosis

Flow cytometry assay was conducted to determine the mechanism of inhibition of U87 survival caused by brucine. As mentioned above, treated or untreated U87 cells were examined by FACS to detect both apoptosis and the cell cycle stage. Figure 2 shows that the rate of cells in G2 was gradually increased with increasing amounts of brucine, specifically at 1.0 mM (Figure 2D) and 0 mM (control; Figure 2A), suggesting that brucine can arrest the cell cycle in U87 cells. Thus, brucine inhibited U87 cell growth. However, as shown in Figure 3, the level of U87 cell apoptosis did not correlate with the dose of brucine in the cells, indicating that brucine suppressed the proliferation of U87 cells rather than killing the cells.

Brucine affects transcription and expression of c-Myb

RT-PCR and western blotting were performed to investigate the effects of brucine on transcription and expression of c-Myb. In RT-PCR, total RNAs of treated or untreated cells were extracted to detect c-Myb transcription. Primers targeting GADPH as an internal reference and c-Myb were designed in-house and then synthesized by Sangon Biotech. The results (Figure 4) showed a negative correlation between the dose of brucine and levels of c-Myb transcripts in U87 cells. Analysis of protein levels (Figure 5) showed a similar downward trend in c-Myb expression in U87 cells with increasing doses of brucine. These results suggest that brucine negatively regulates the expression of c-Myb through a direct or indirect pathway.

A dual-luciferase reporter assay was used to examine whether brucine acts directly on G-quadruplexes located in the promoter region of c-Myb. The promoter region of pGL3, 5'-GAGCTCTTACGCGT-3', which did not contain sufficient guanines to form a G-quadruplex structure, was replaced by the guanine-rich sequence at the c-Myb promoter region. Cells were transfected with the modified pGL3 (pGL3-p or pGL3-basic) vectors. Comparison of the two untreated groups (Figure 6A) showed that pGL3-p expression was remarkably increased relative to pGL3-basic, indicating that the guanine-rich sequence with a potential to form G-quadruplexes significantly increased vector expression. The degree of influence of this sequence is represented by the pGL3-p/pGL3-basic ratio under the same treatment conditions. As shown in Figure 6B, the ratios increased with increasing concentrations of brucine. In contrast, the expression of pGL3-basic was not increased. This demonstrates that the guanine-rich sequence in the promoter region of pGL3-basic was the only or at least the most effective target of brucine. Therefore, brucine may have functioned by targeting the guanine-rich sequence of the c-Myb promoter and enhanced its effect on the expression of pGL3 in our experiment.

Brucine binds G-quadruplexes to inhibit formation of double-stranded DNA

ESI-MS was used to investigate whether brucine binds G-quadruplexes in the c-Myb promoter region. The approximate molecular weights of S1, S2, double-stranded S1 and S2 (S1+S2), and brucine are 5693, 5311, 11004, and 394; therefore, the peak of a certain number in Figure 7 shows the content of a specific particle with a molecular weight of this certain number. For instance, the peak of 6087 represented S1 with a molecule of brucine binding (S1+1b) and peak of 6876 represented S1 with 3 molecules of brucine (S1+3b). The process of annealing may help S1 and S2 to form secondary structures such as G-quadruplexes and double-stranded structures. Without the annealing process, the results of group A and C showed that only a very small amount of S1 was combined with brucine in a ratio of 1:1 and the quantity of double-stranded DNA was difficult to detect. Compared to the results of group A2-4, group B2-4 had peaks of S1+2b to S1+5b and higher peaks of S1+1b, suggesting that brucine molecules were more likely to bind to a secondary structure of the guanine-rich S1, specifically G-quadruplexes of S1, rather than a “line-like” S1. D1 showed some formation of double-stranded S1+S2 without brucine rather than C1. However, there are nearly no S1+S2 peaks, but rather peaks of S1+1b to S1+5b in D2-4, suggesting that brucine disturbs the formation of S1+S2 by binding to G-quadruplexes of S1.

Effect of brucine on the cell cycle and apoptosis are related to genes in U87 cells

The results of MTT and flow cytometry revealed that at brucine concentration of 1.0 mM, the proliferation of U87 cells decreased without an increase cell death. To understand this phenomenon, western blotting was performed to determine the effects of brucine on protein levels of cell cycle-related cyclin D1 and apoptosis-related BAX, caspase-3, and caspase-9. Cyclin D1 levels gradually decreased with increasing doses of brucine; however, levels of BAX, caspase-3, and caspase-9 were not significantly affected by the treatment with brucine (Figure 5). These results validated the flow cytometry results.

Brucine suppresses U87 cell growth *in vivo*

To determine whether brucine has antitumor effects on U87 cells both *in vitro* and *in vivo*, we established a U87 xenograft model in female nude mice. Two weeks after injection of equal amounts of U87 cells, tumors were palpable in all mice. The mice were separated into brucine therapy and NS control groups, and all mice remained alive throughout treatment. Changes in tumor size in the two groups were calculated using the formula $tumor\ volume = 1/2 \times length \times width^2$(21). The results, shown in Figure 8B, indicated that the average tumor size in the brucine treatment group increased more slowly than that in the control group. Images (Figure 8A) of tumors resected on the last day of treatment revealed the effects of brucine on U87 tumors. Furthermore, immunohistochemistry was performed to assess the expression of Ki-67 and c-Myb in the tumors, and the amounts of both Ki-67 and c-Myb in the brucine treatment group were lower than those in the control group (Figure 8C). Therefore, brucine has therapeutic effects when used to treat U87 tumors in a xenograft model.

Discussion

Glioblastomas are one of the deadliest and chemotherapy-resistant malignancies of the central nervous system. In this study, brucine was shown to inhibit the proliferation of U87 glioblastoma cells both *in vitro* and *in vivo*. Other studies of brucine indicated that the mechanisms underlying its anti-tumor effects include cell cycle arrest and induction of apoptosis in cancers such as hepatocellular carcinoma (22), multiple myeloma (23), and colon cancer (24). However, in our study, brucine treatment at a concentration of 1.0 mM did not significantly induce the apoptosis of U87 cells *in vitro*, suggesting that brucine fights different tumors through different pathways, or that U87 cells are not as sensitive to brucine as other cancer cells, particularly in term of the susceptibility to apoptosis. Although increasing the concentration of brucine may increase the impact of apoptosis on U87 cells, we maintained a low brucine dose because of its considerable toxicity (intravenous toxicity of brucine in mice: LD_{50} = 13.17 mg/kg, LD_5 = 9.17 mg/kg) (25). Moreover, we chose a relatively safe dose of 10 mg/kg brucine for intraperitoneal delivery in the *in vivo* study. No mice died from brucine toxicity. The data on tumor sizes in the *in vivo* assay demonstrated the therapeutic effect of brucine on U87 tumors. In addition, immunohistochemistry of the tumors revealed reduced c-Myb protein levels in the brucine treatment group. Combined with the results of RT-PCR and western blotting, c-Myb appears to play an important role in the mechanism underlying the effects of brucine on U87 cells.

Parallel G-quadruplexes structures in various genes form based on their unique DNA sequences and interact with specific proteins or small molecules(13). The same sequence can form the same G-quadruplexes and interact with same molecules in different genes. In our ESI-MS assay, brucine bound to the secondary structure of S1, G-quadruplexes, and blocked the formation of double-stranded DNA of S1 and S2. Typically, it is difficult for a guanine-rich sequence to form double-stranded DNA with its complementary strand because of the formation of G-quadruplexes in the annealing process. Brucine enhances the formation of G-quadruplexes to amplify this issue, affecting the transcription of specific genes. However, in our dual luciferase assay, although brucine targeted the specific guanine-rich sequence from the c-Myb promoter, its effects on G-quadruplexes in c-Myb and pGL3-p were completely

different: brucine inhibited c-Myb and functioned as an agonist of pGL3-p. In addition, only the guanine-rich sequence in the pGL3-p promoter enhanced plasmid expression compared to that in pGL3-basic without brucine treatment. This may be because of the different positions of G-quadruplexes in their DNA, different transcription factors associated with c-Myb and pGL3, and different proto-oncogene and pGL3 plasmid sequences. Further studies of the function of different G-quadruplexes in plasmids and non-oncogenes are needed to resolve these differences.

Furthermore, this study showed that the oncogene c-Myb in U87 cells is inhibited by interactions between brucine and G-quadruplexes in the c-Myb promoter to reduce the proliferation of these cells *in vitro*. This suggests that other ligands targeting the same structure have a similar glioblastoma cell anti-tumor effect. For example, dehydrocorydaline showed greater binding affinity and selectivity for c-Myb G-quadruplexes than brucine(26). Thus, dehydrocorydaline is another potential anti-tumor drug for glioblastoma, and may be more effective and selective, and less toxic than brucine. However, to date, no study has demonstrated the therapeutic effects of dehydrocorydaline on glioblastomas. We propose that the therapeutic efficiency and safety of dehydrocorydaline for glioblastoma treatment should be investigated for their comparison with these features of brucine.

Conclusions

Brucine is an effective suppressor of glioblastoma U87 cells both *in vitro* and *in vivo*. For U87 cells, cell cycle arrest and reduction in the expression of oncogene c-Myb was achieved by targeting G-quadruplexes located in the c-Myb promoter region. This is an important therapeutic mechanism of brucine. This suggests that brucine is an effective therapy for glioblastoma.

Abbreviations

OD, optical density; PI, propidium iodide; ESI-MS, electrospray ionization mass spectrometry; NS, normal saline

Declarations

Funding

This work was supported by the National Nature and Science Foundation of China (81772684), Scientific Research Foundation of Jilin province (20160101086JC), Research and Planning Project of the 13th Five-Year Science and Technology Project of Jilin Provincial Department of Education (JJKH20180191KJ), and Interdisciplinary Innovation Project of First Hospital of Jilin University (JDYYJC001).

Competing interests

The authors declare that they have no competing interests.

Ethical approval and consent to participate

All procedures involving animal participants were performed in accordance with the ethical standards of the Ethics Committee of the First Hospital of Jilin University and its institutional animal-care committee.

Availability of data and materials

The datasets supporting the conclusions of this article are included within the article.

Acknowledgements

Not applicable

Consent for publication

Not applicable

Authors' information

Affiliations

Department of Neurosurgery, the First Hospital of Jilin University, Jilin University, Changchun, 130000, China

Qiaochu Liu, Qunhui Wang, Chuanqi Lv, Ziqiang Liu, Haijun Gao, Yong Chen, Gang Zhao

Department of Neurology, The First Affiliated Hospital of Harbin Medical University, Harbin Medical University, Harbin, 150000, China

Di Huo

Authors' contributions

Qiaochu Liu was the designer this study, the main write of the manuscript and involved in all parts of the experiments. Gang Zhao and Yong Chen raised funds and revised the manuscript. Other authors separately participated into the running of the experiments.

References

1. Jacobs JF, Idema AJ, Bol KF, Nierkens S, Grauer OM, Wesseling P, et al. Regulatory T cells and the PD-L1/PD-1 pathway mediate immune suppression in malignant human brain tumors. Neuro-oncology. 2009;11(4):394-402.
2. Ostrom QT, Bauchet L, Davis FG, Deltour I, Fisher JL, Langer CE, et al. The epidemiology of glioma in adults: a "state of the science" review. Neuro-oncology. 2014;16(7):896-913.
3. Louis DN, Perry A, Reifenberger G, von Deimling A, Figarella-Branger D, Cavenee WK, et al. The 2016 World Health Organization Classification of Tumors of the Central Nervous System: a summary. Acta

neuropathologica. 2016;131(6):803-20.
4. Weller M, van den Bent M, Tonn JC, Stupp R, Preusser M, Cohen-Jonathan-Moyal E, et al. European Association for Neuro-Oncology (EANO) guideline on the diagnosis and treatment of adult astrocytic and oligodendroglial gliomas. The Lancet Oncology. 2017;18(6):e315-e29.
5. Stupp R, Mason WP, van den Bent MJ, Weller M, Fisher B, Taphoorn MJ, et al. Radiotherapy plus concomitant and adjuvant temozolomide for glioblastoma. The New England journal of medicine. 2005;352(10):987-96.
6. Masui K, Cloughesy TF, Mischel PS. Review: molecular pathology in adult high-grade gliomas: from molecular diagnostics to target therapies. Neuropathology and applied neurobiology. 2012;38(3):271-91.
7. Oh IH, Reddy EP. The myb gene family in cell growth, differentiation and apoptosis. Oncogene. 1999;18(19):3017-33.
8. Beug H, von Kirchbach A, Döderlein G, Conscience JF, Graf T. Chicken hematopoietic cells transformed by seven strains of defective avian leukemia viruses display three distinct phenotypes of differentiation. Cell. 1979;18(2):375-90.
9. Bell D, Roberts D, Karpowicz M, Hanna EY, Weber RS, El-Naggar AK. Clinical significance of Myb protein and downstream target genes in salivary adenoid cystic carcinoma. Cancer biology & therapy. 2011;12(7):569-73.
10. Welter C, Henn W, Theisinger B, Fischer H, Zang KD, Blin N. The cellular myb oncogene is amplified, rearranged and activated in human glioblastoma cell lines. Cancer letters. 1990;52(1):57-62.
11. Ramsay RG, Gonda TJ. MYB function in normal and cancer cells. Nature reviews Cancer. 2008;8(7):523-34.
12. Lei W, Liu F, Ness SA. Positive and negative regulation of c-Myb by cyclin D1, cyclin-dependent kinases, and p27 Kip1. Blood. 2005;105(10):3855-61.
13. Yang D. G-Quadruplex DNA and RNA. Methods in molecular biology (Clifton, NJ). 2019;2035:1-24.
14. Grand CL, Powell TJ, Nagle RB, Bearss DJ, Tye D, Gleason-Guzman M, et al. Mutations in the G-quadruplex silencer element and their relationship to c-MYC overexpression, NM23 repression, and therapeutic rescue. Proceedings of the National Academy of Sciences of the United States of America. 2005;102(2):516.
15. Rhodes D, Lipps HJ. G-quadruplexes and their regulatory roles in biology. Nucleic acids research. 2015;43(18):8627-37.
16. Eddy J, Maizels N. Gene function correlates with potential for G4 DNA formation in the human genome. Nucleic acids research. 2006;34(14):3887-96.
17. Haider S, Parkinson GN, Marsh TC. G-Quadruplexes (GQU). Journal of nucleic acids. 2018;2018:1079191.
18. Palumbo SL, Memmott RM, Uribe DJ, Krotova-Khan Y, Hurley LH, Ebbinghaus SW. A novel G-quadruplex-forming GGA repeat region in the c-myb promoter is a critical regulator of promoter

activity. Nucleic acids research. 2008;36(6):1755-69.
19. Francisco AP, Paulo A. Oncogene Expression Modulation in Cancer Cell Lines by DNA G-Quadruplex-Interactive Small Molecules. Current medicinal chemistry. 2017;24(42):4873-904.
20. Li H, Hai J, Zhou J, Yuan G. Exploration of binding affinity and selectivity of brucine with G-quadruplex in the c-myb proto-oncogene by electrospray ionization mass spectrometry. Rapid communications in mass spectrometry : RCM. 2016;30(3):407-14.
21. Naito S, von Eschenbach AC, Giavazzi R, Fidler IJ. Growth and metastasis of tumor cells isolated from a human renal cell carcinoma implanted into different organs of nude mice. Cancer research. 1986;46(8):4109-15.
22. Saraswati S, Alhaider AA, Agrawal SS. Anticarcinogenic effect of brucine in diethylnitrosamine initiated and phenobarbital-promoted hepatocarcinogenesis in rats. Chemico-biological interactions. 2013;206(2):214-21.
23. Rao PS, Ramanadham M, Prasad MN. Anti-proliferative and cytotoxic effects of Strychnos nux-vomica root extract on human multiple myeloma cell line - RPMI 8226. Food and chemical toxicology : an international journal published for the British Industrial Biological Research Association. 2009;47(2):283-8.
24. Zheng L, Wang X, Luo W, Zhan Y, Zhang Y. Brucine, an effective natural compound derived from nux-vomica, induces G1 phase arrest and apoptosis in LoVo cells. Food and chemical toxicology : an international journal published for the British Industrial Biological Research Association. 2013;58:332-9.
25. Chen J, Yan GJ, Hu RR, Gu QW, Chen ML, Gu W, et al. Improved pharmacokinetics and reduced toxicity of brucine after encapsulation into stealth liposomes: role of phosphatidylcholine. International journal of nanomedicine. 2012;7:3567-77.
26. Cui X, Yuan G. Formation and recognition of G-quadruplex in promoter of c-myb oncogene by electrospray ionization mass spectrometry. Journal of mass spectrometry : JMS. 2011;46(9):849-55.

Figures

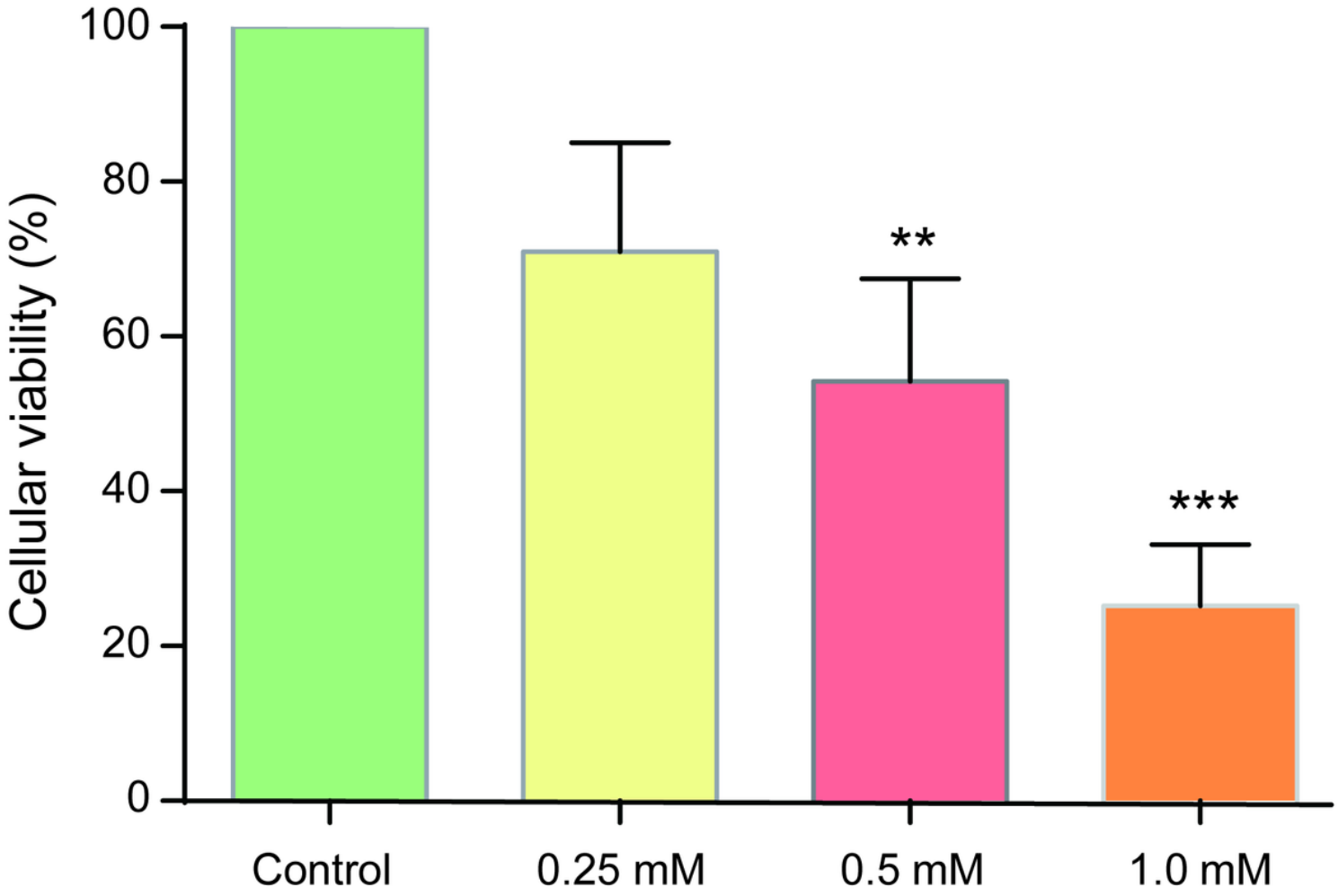

Figure 1

Brucine inhibited viability of U87 cells. U87 cells were seeded into a 96-well plate and treated with brucine at different concentrations for 24 h. Next, the cells were assessed by MTT assay. Cell viability is represented by the OD 450 nm values shown in the figure. The overall results are presented as the mean ± SD and analyzed using one-way ANOVA test and $P < 0.0001$. Each treating group was separately compared to the control group and analyzed by t test (1.0 mM vs. control: $P = 0.0004$; 0.5 mM vs. control: $P = 0.0064$).

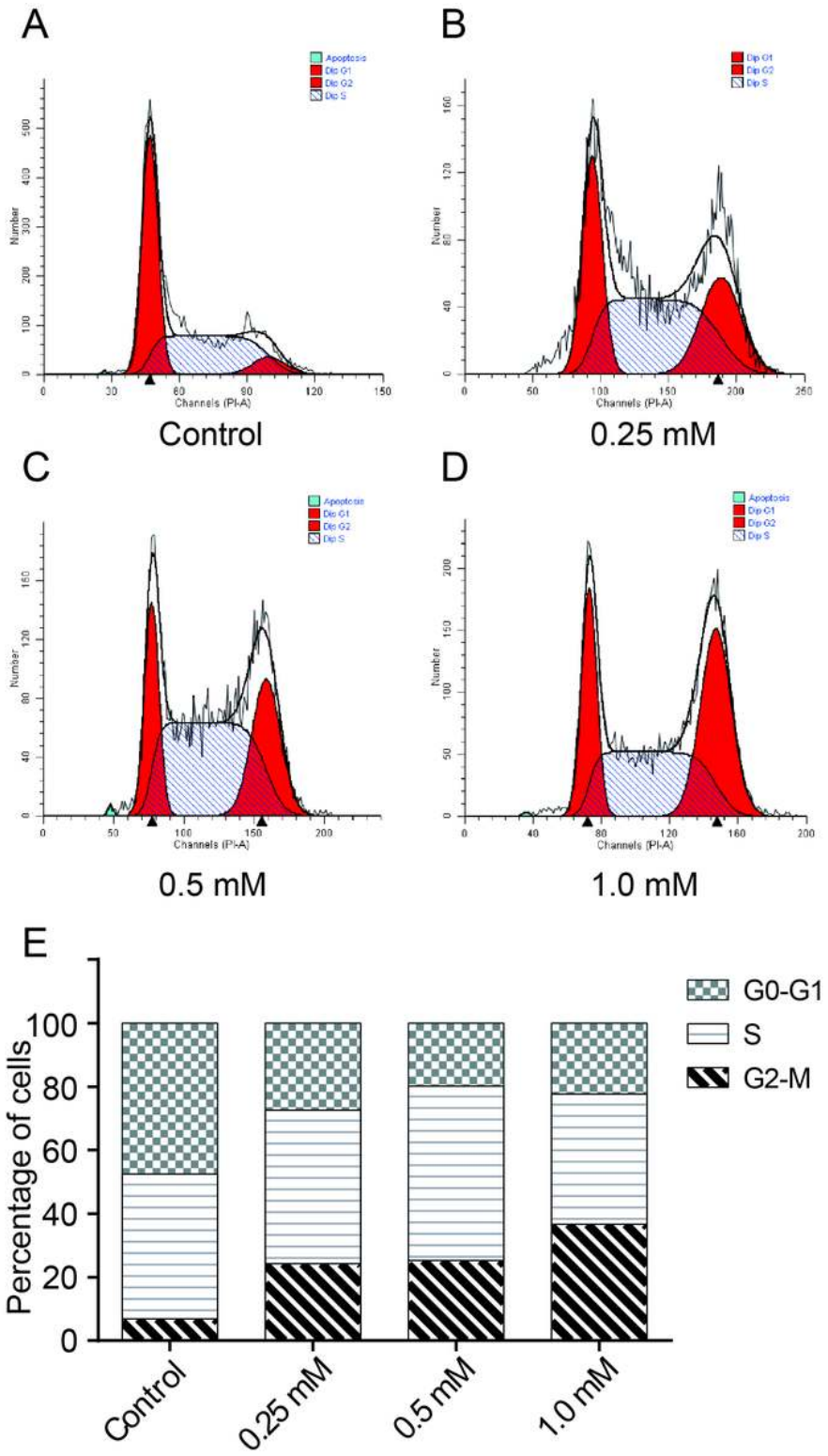

Figure 2

Brucine arrested the cell cycle of U87 cells. U87 cells were seeded into a 6-well plate and treated with brucine at different concentrations for 24 h. The harvested cells were washed with PBS and 70% alcohol was added. The cells were washed again with PBS and stained with propidium iodide in the presence of 100 μL of RNase A for 30 min. Data were collected by flow cytometry.

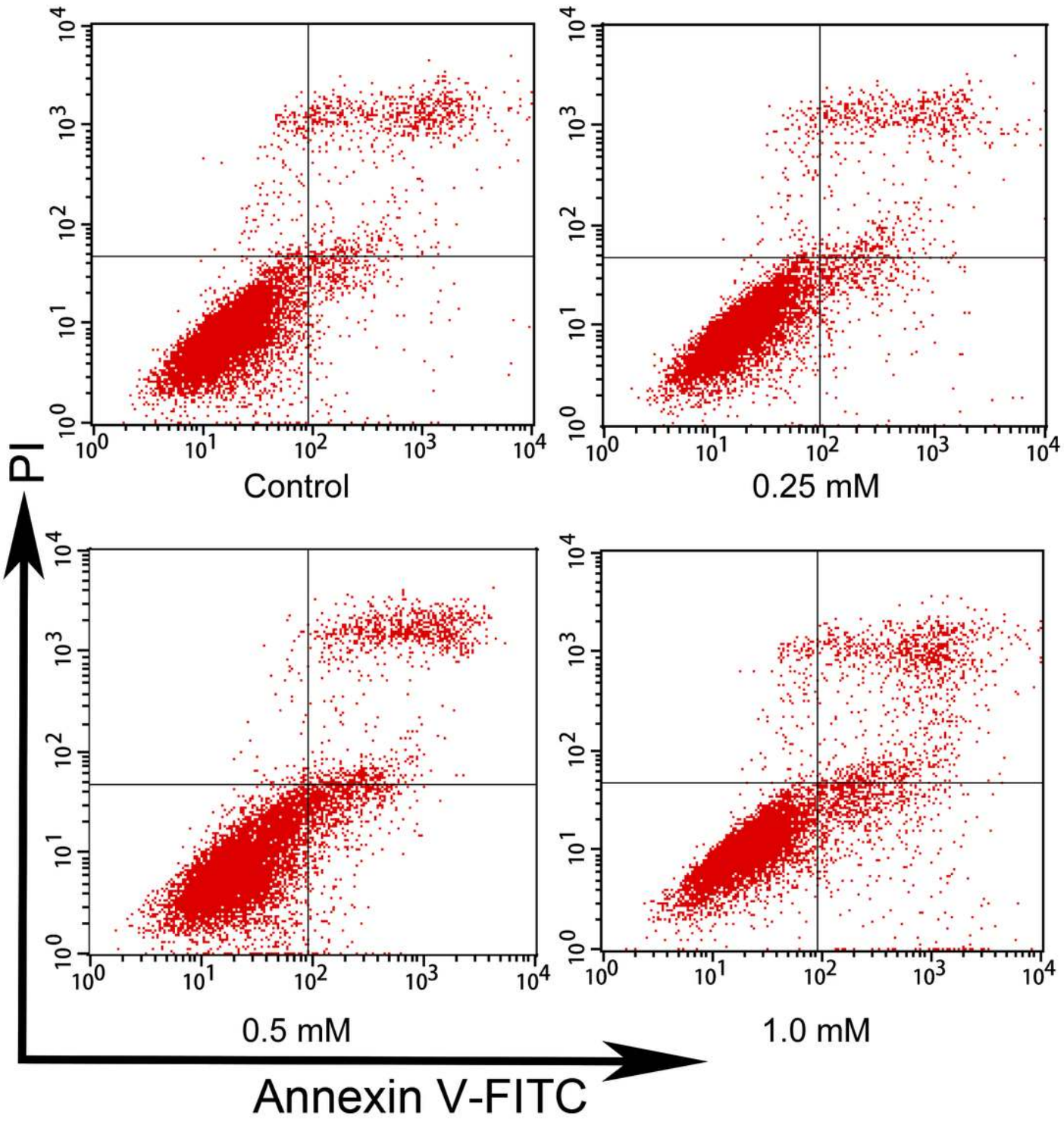

Figure 3

Effect of brucine on apoptosis of U87 cells. U87 cells were seeded into a 6-well plate and treated with brucine at different concentrations for 24 h. The harvested cells were washed with PBS and 1× binding buffer (100 μL) was added to each sample. Cells were stained with Annexin V/PI before analysis by flow cytometry within 1 h.

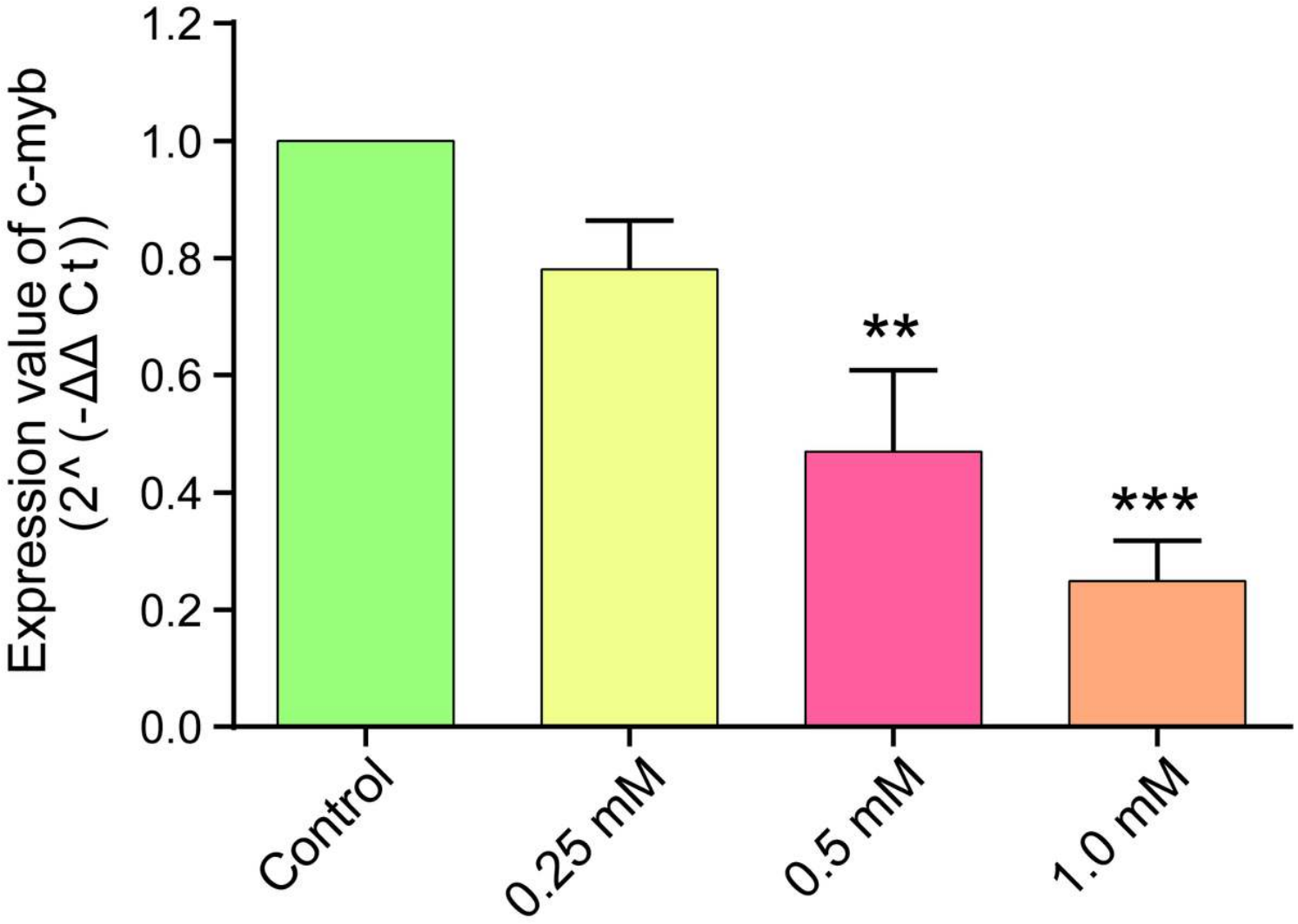

Figure 4

Brucine reduced transcription of c-Myb. U87 cells were treated with different concentrations of brucine and incubated for 24 h before their total RNA was extracted. GADPH was used as internal reference. Values of each treated group 2-ΔΔCT are presented as the mean ± SD and analyzed by one-way ANOVA, and $P < 0.01$.

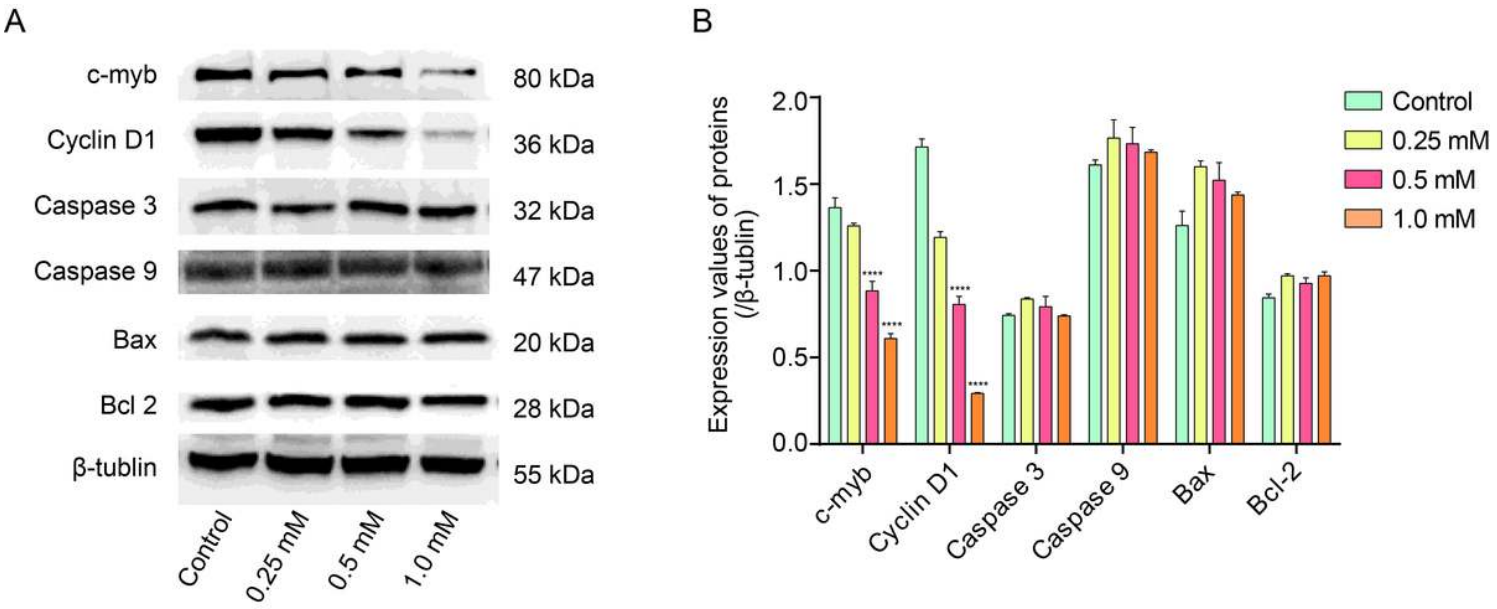

Figure 5

Effect of brucine on c-Myb, Cyclin D1, Bcl-2, Caspase 3, Caspase 9, and BAX proteins. The expression level of the indicated protein in U87 cells from each group was detected by western blotting. β-Tubulin was used as an internal reference. The western blot gels are shown in A and statistical data are presented as the mean ± SD in B.

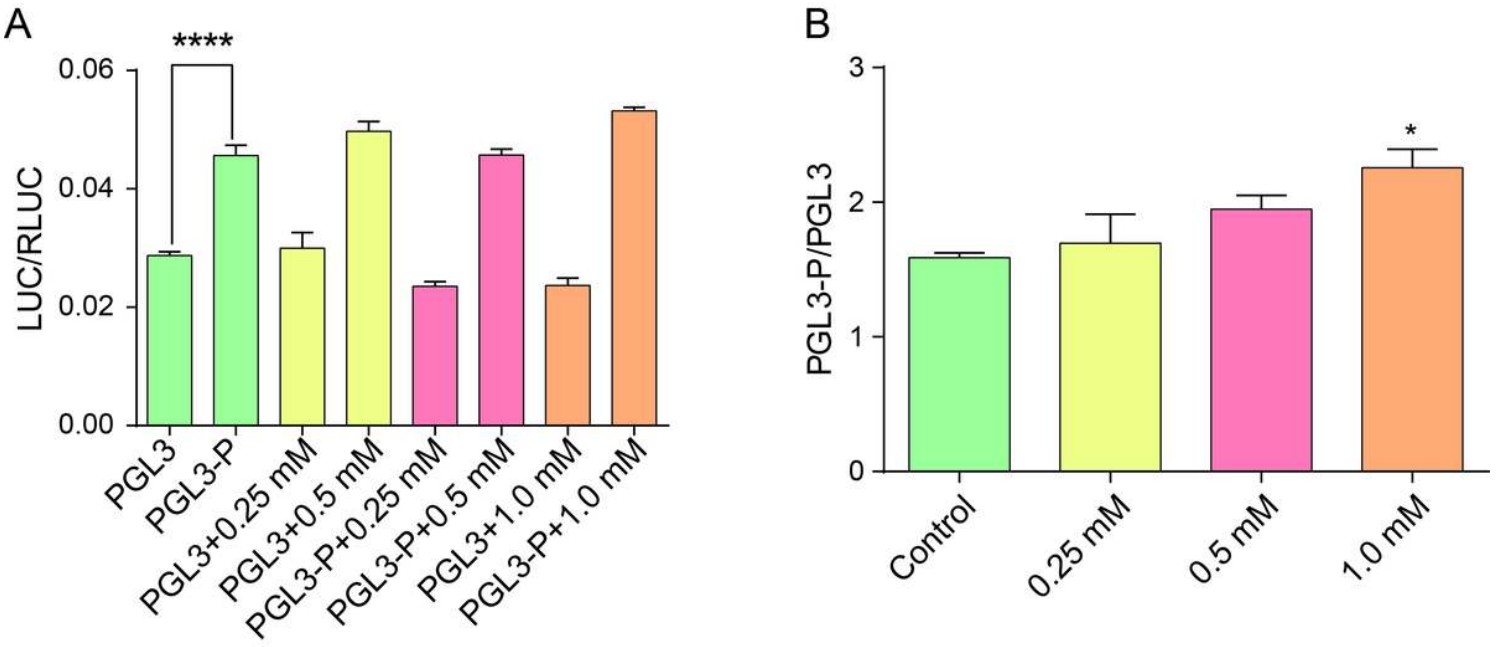

Figure 6

Effect of brucine on the guanine-rich sequence located in the c-Myb promoter region. The guanine-rich sequence in the c-Myb promoter region was synthesized to replace the sequence from site KpnI to NheI of pGL3-basic. Cells (n=293) were transfected with pGL3-p or pGL3 and then treated with different concentrations of brucine for 24 h. pRL-SV40 was used as an internal reference. The results of LUC/RLUC

(A) showed the levels of the guanine-rich sequence and brucine affecting the plasmid expression and the result of pGL3-p/pGL3 (B) represented how much the brucine influenced the guanine-rich sequence. The data are presented as the mean ± SD and analyzed by one-way ANOVA.

Figure 7

Brucine binds G-quadruplexes to inhibit the formation of double-stranded DNA. The guanine-rich sequence of c-Myb promoter, S1, and its complementary strand, S2, were grouped and added to annealing buffer. Samples were mixed with different concentrations of brucine and groups B and D were subject to the annealing process. Data were detected with a Waters SYNAPT G2-Si. The X-axis represents the molecular weights of the granules detected and the Y-axis represents the ratios of the granules' quantities.

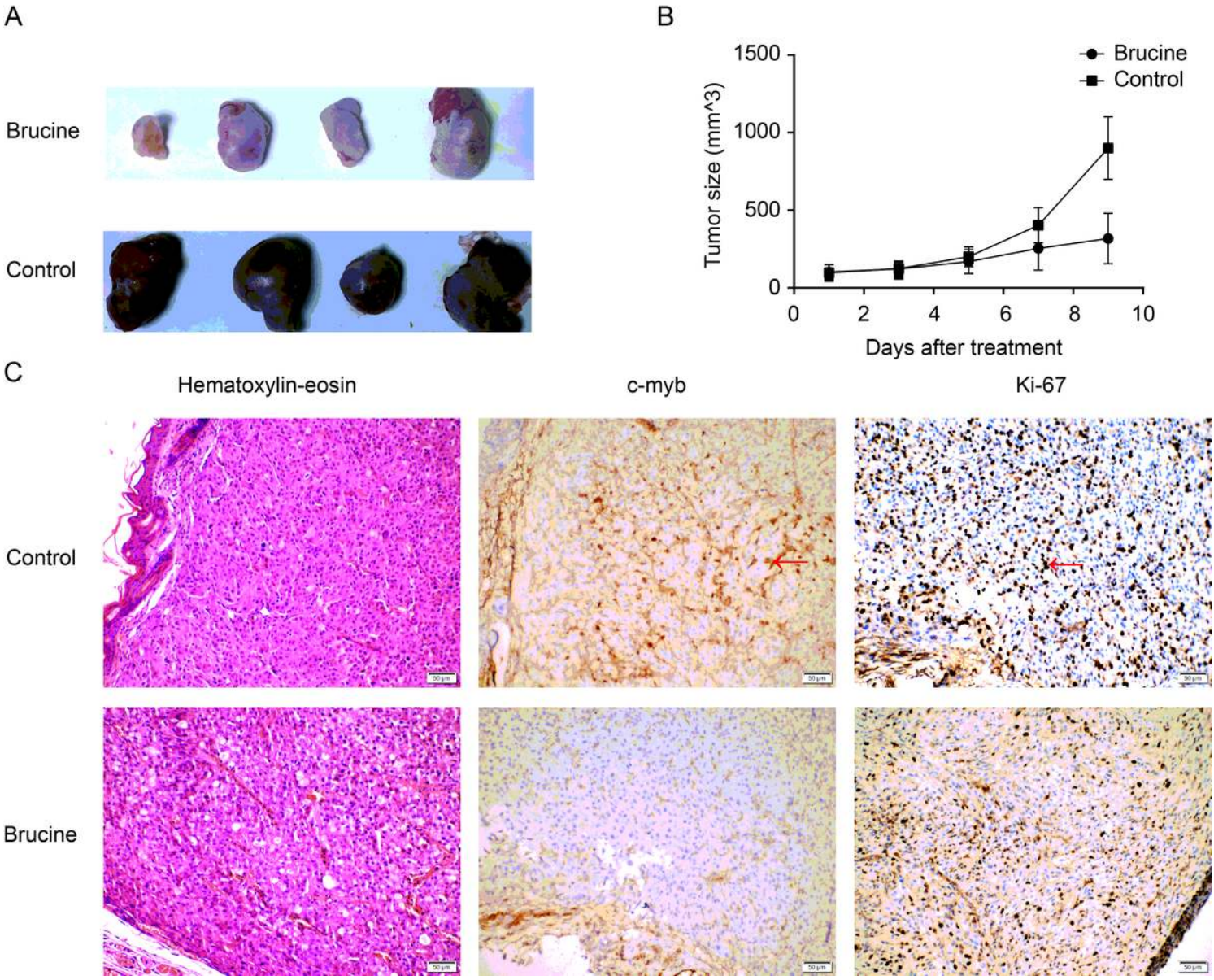

Figure 8

Brucine suppressed U87 tumors in vivo. U87 cells were injected into nude mice to establish an in vivo model. After tumor growth in all mice, they were separated into two groups and treated with brucine or NS. The changes in tumor sizes are shown (B) as the mean ± SD and the resected tumors are shown in (A). The expression levels of Ki-67 and c-Myb in tumor were detected by immunohistochemistry and images were captured at 200× magnification (C).